Late Variscan, Permo-Carboniferous, Al-K plutonism in the South Portuguese Zone: El Crispinejo cordierite-bearing granite

A. DÍEZ-MONTES[1]   P. VALVERDE-VAQUERO[2]   C. REY-MORAL[2]   T. SÁNCHEZ-GARCÍA[3]

[1]Instituto Geológico y Minero de España, IGME
C/ Azafranal, 48, 37001-Salamanca, Spain.   Díez-Montes E-mail: al.diez@igme.es

[2]Instituto Geológico y Minero de España, IGME
C/ La Calera, 28760-Tres Cantos, Spain.   Valverde-Vaquero E-mail: p.valverde@igme.es
Rey-Moral E-mail: c.rey@igme.es

[3]Instituto Geológico y Minero de España, IGME
C/ Ríos Rosas, 23, 28003-Madrid, Spain.   Sánchez-García E-mail: t.sanchez@igme.es

┤ **A B S T R A C T** ├

The El Crispinejo granite forms part of a small, but distinctive late intrusive suite of cordierite-bearing peraluminous granites in the South Portuguese Zone (SPZ). This granite has the best outcrop relationships of the suite. It cross-cuts different members of the Sierra Norte Batholith of the SPZ and the Carboniferous Volcano-Sedimentary Complex of the Iberian Pyrite Belt, producing contact metamorphism. This late pluton has a high K content which results in a contrasting geophysical response (K-Th-U) with respect to the surrounding trondhjemitic granitoids of the TTG suite of the Sierra Norte Batholith. A concordant monazite-zircon U-Pb ID-TIMS age of 300.5 +0.5/-1.5Ma demonstrates Permo-Carboniferous age for this late Variscan magmatic event. The granite is associated with a series of ore showings (F-Pb-Zn and Sn-W) which are completely different from the nearby, massive sulphide and manganese ore deposits of the Iberian Pyrite Belt, indicating the unique character of this intrusion.

KEYWORDS | **South Portuguese Zone. Iberian Pyrite Belt. El Crispinejo granite. Radiometric. U-Pb ID-TIMS geochronology.**

INTRODUCTION

The South Portuguese Zone (SPZ; Fig 1) of the Iberian Massif (*e.g.* Oliveira, 1990) hosts a large composite batholith known as the Sierra Norte Batholith (Simancas, 1981, 1983; de la Rosa, 1992). This batholith is formed essentially by a 350-335Ma tonalite-trondhjemite-granodiorite (TTG) association, (Schütz *et al.*, 1987; Dunning *et al.*, 2002; Barrie *et al.*, 2002; Díez-Montes and Bellido Mulas, 2008). The granitoids of the TTG association are intruded by a discrete group of potassic – aluminous granites such as El Berrocal and El Crispinejo intrusions (Díez-Montes

and Bellido Mulas, 2008). In contrast to other members of the Sierra Norte Batholith, these late granites do not display a subvolcanic texture, but instead show porphyritic textures with K-feldspar megacrysts. The granites are peraluminous as evidenced by the presence of cordierite. They show a very contrasting radiometric geophysical signature. In addition to intruding on the trondhjemitic granitoids, they also cross-cut folds and have produced contact metamorphism in the Devonian-Carboniferous Volcano-Sedimentary Complex of the Iberian Pyrite Belt (*e.g.* Oliveira, 1990; Díez-Montes and Bellido Mulas, 2008). These field relationships suggest that these granites constitute a separate, late

intrusive event, however their age is not known with precision. The mineralization associated with these intrusions is also different from the classic massive sulphide deposits of the SPZ (*e.g.* Barrie *et al.*, 2002), and more akin to that observed in peraluminous S-type granite suites such as those of the Central Iberian Zone.

The El Crispinejo granite has clear intrusive relationships with the surrounding units and one of the best outcrop exposures of the suite. This paper provides a detailed description of the different facies of the granite, as well as geochemical data and geophysical images to show the contrasting signature of this granite with respect to the surrounding intrusions of the Sierra Norte Batholith. New U-Pb geochronology demonstrates that this granite is part of a Late Variscan intrusive event, 50Ma younger than the classic ~350Ma plutonism the SPZ.
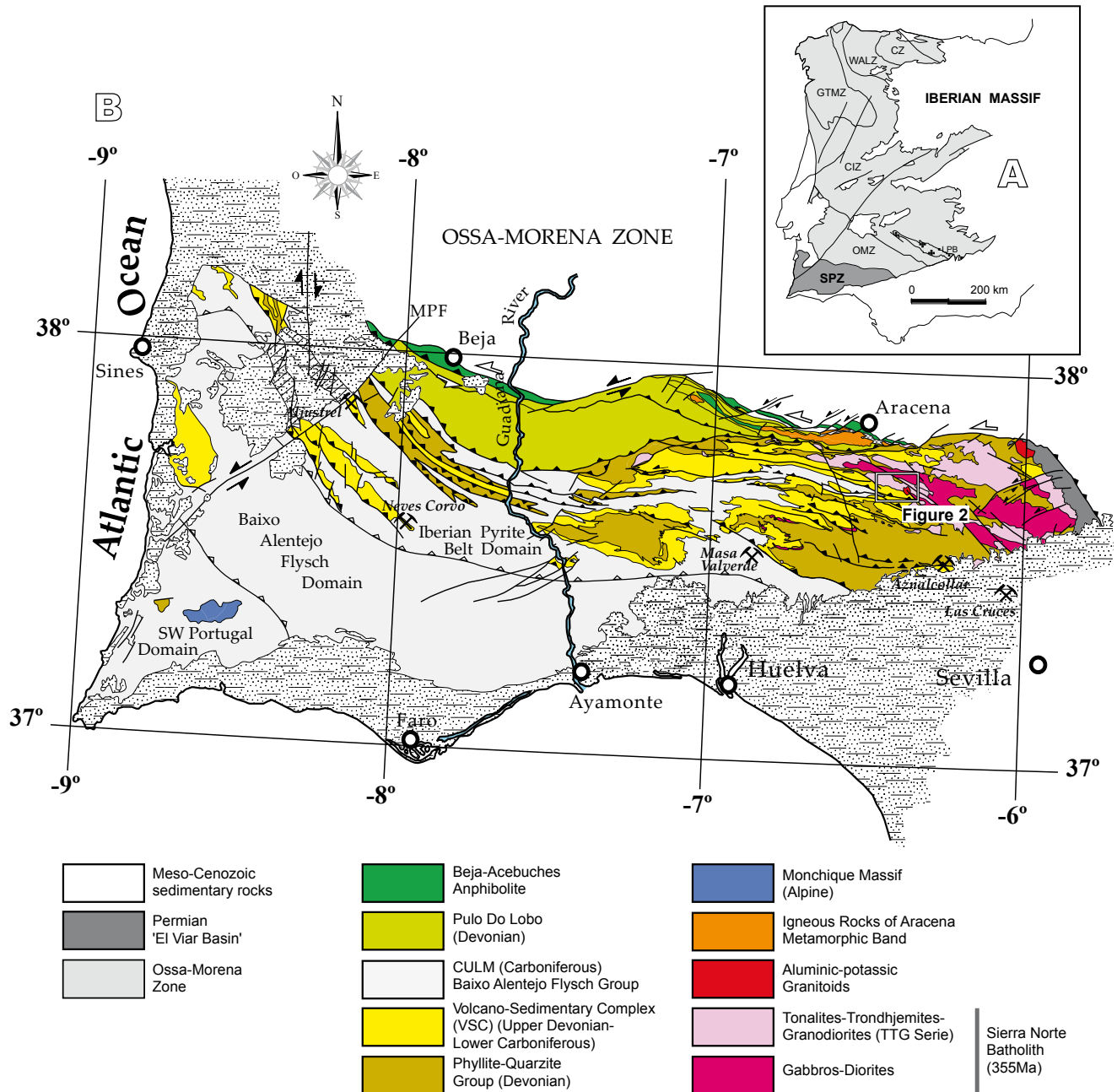

FIGURE 1. A) Division of the Iberian Massif according to Lotze (1945) with the location of the South Portuguese Zone (SPZ) within the Iberian Massif. OMZ, Ossa-Morena Zone. CIZ, Central Iberian Zone. LPB, Los Pedroches Batholith. GTMZ, Galicia-Trás-os-Montes Zone. WALZ, West Asturian-Leonese Zone. CZ, Cantabrian Zone. B) Geological map of the South Portuguese Zone (modified from IGME, 1994).
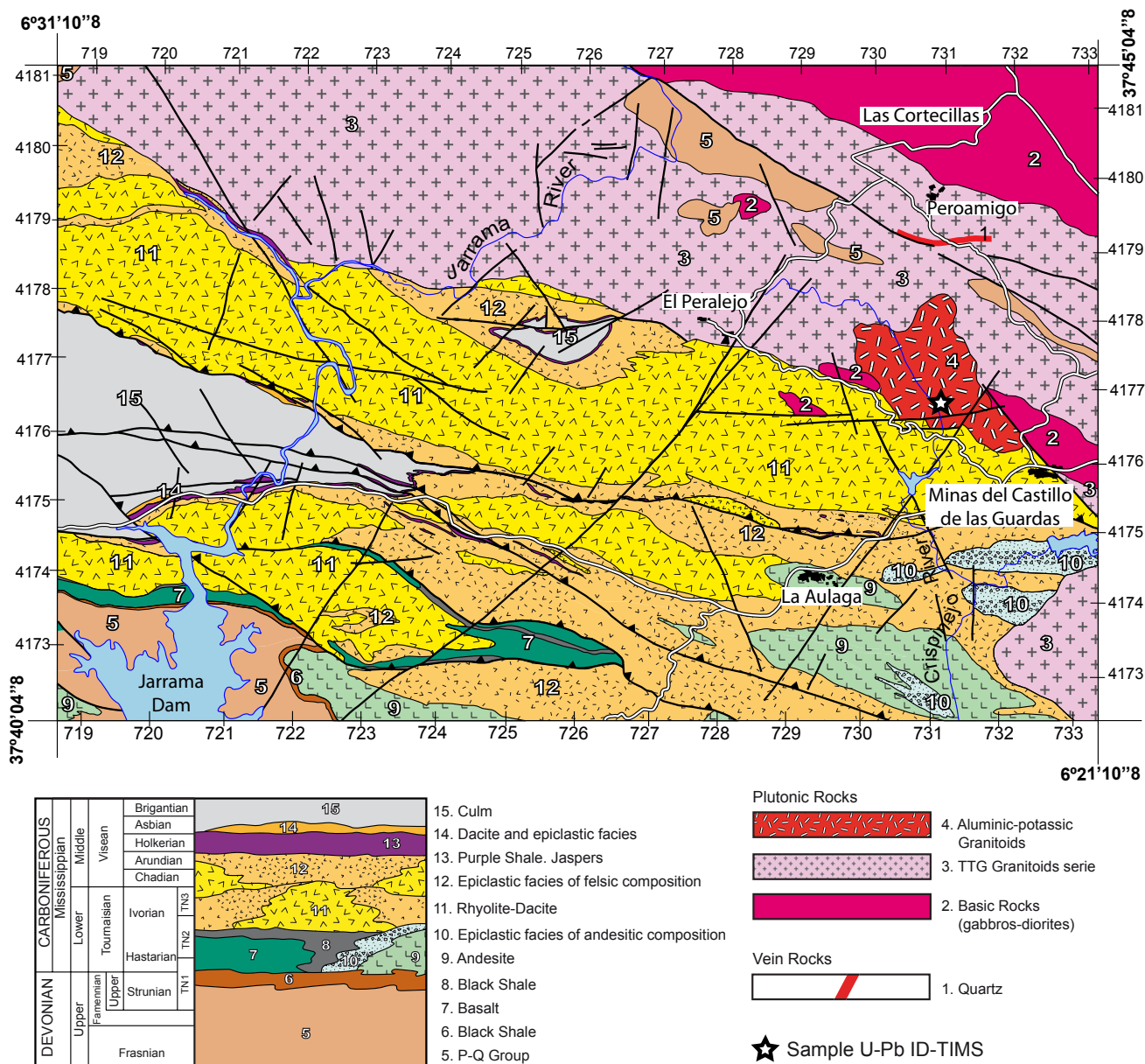
FIGURE 2. Geological map from Díez-Montes *et al.* (1999) of the Minas del Castillo de las Guardas area showing the location of the El Crispinejo granite. Coordinate system: international ellipsoid, European datum, UTM coordinates. Coordinates of sample U-Pb ID-TIMS, X=731.115, Y=4.176.513.

GEOLOGICAL SETTING

The South-Portuguese Zone (SPZ) constitutes the southern foreland of the Iberian Massif (*e.g.* Oliveira, 1990). This external zone has been correlated with the Rheno-Hercynian Zone of the Variscan Belt in Belgium and Germany and with the Variscan foreland of the British Isles (Oliveira *et al.*, 1979; Franke, 1992; von Raumer *et al.*, 2003). According to Oliveira (1990), the SPZ is divided into five major domains, from north to south: Beja-Acebuches "ophiolitic" domain, Pulo do Lobo antiform, Iberian Pyrite Belt domain, Flysch of Baixo Alentejo, and SW Portugal (Bordeira and Aljeruz antiforms).

Our area of study lies within the Iberian Pyrite Belt domain. This domain is subdivided into two separate units, the intrusive Sierra Norte Batholith (SNB) and Iberian Pyrite Belt (IPB), *ss*. The IPB contains the oldest stratigraphic units of the South Portuguese Zone. It is made (Schemerhon, 1971) of three major units: the Phyllite-Quartzite Group (PQG), the Volcano-Sedimentary Complex (VSC), and the Culm Group (CG). The oldest unit corresponds to the Devonian
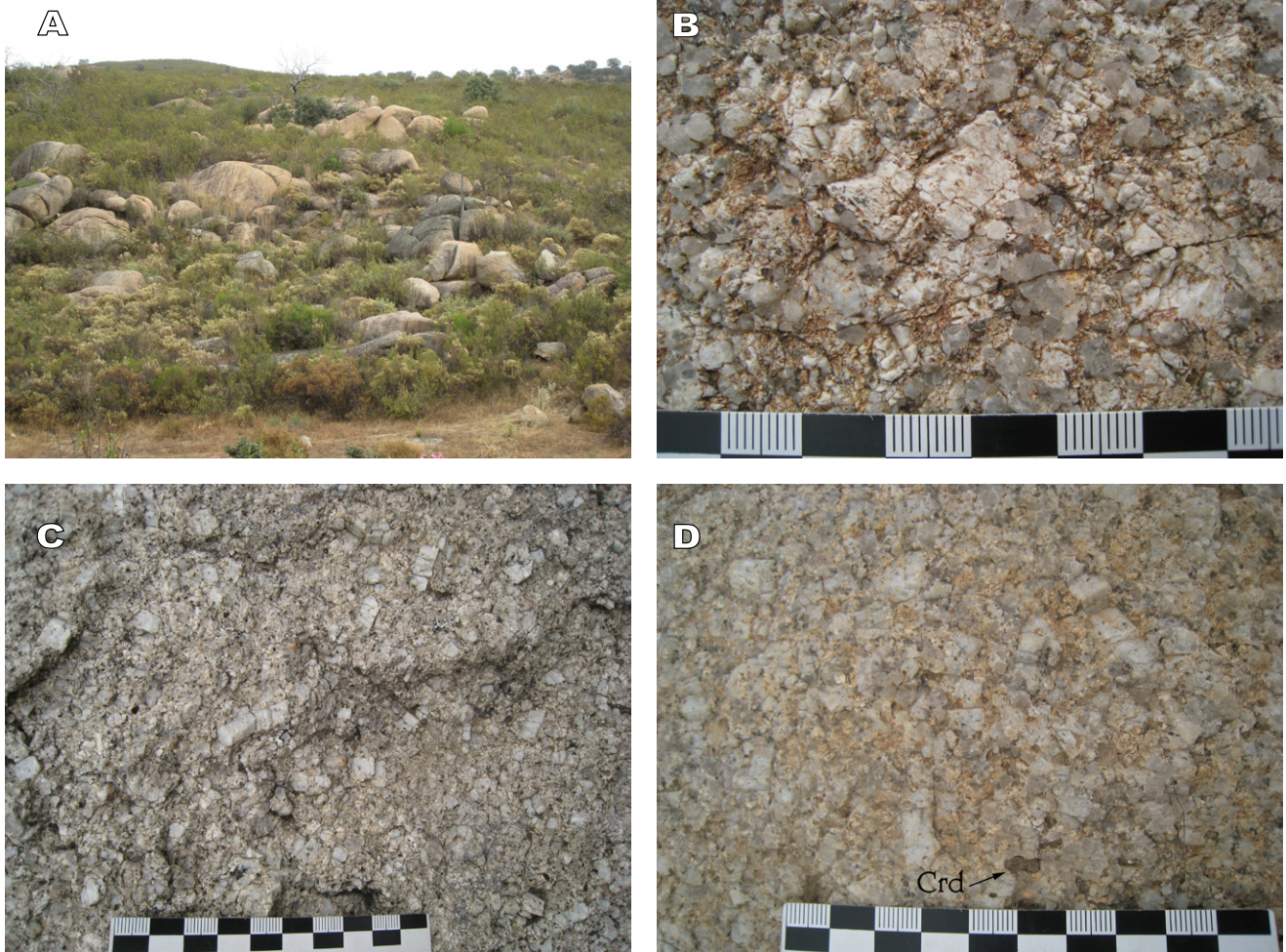
FIGURE 3. Outcrop and macroscopic aspect of the El Crispinejo granite. A) General outcrop, boulder field characteristic of the coarse-grained granite. B) Macroscopic texture of granite with large quartz and feldspar crystals (scale major unit: cm, minor unit: mm). C) Porphyritic facies with K-feldspar megacrysts. D) Macroscopic texture of granite with cordierite prisms (Crd).

shales, sandstones, greywackes, quartzites and minor conglomerates of the PQG. The VSC is Upper Devonian to Lower Carboniferous in age and consists of a submarine volcano-siliciclastic sequence with abundant basalt, dacite and rhyolite intercalated with volcano-sedimentary and epiclastic rocks, sandstone, shale and red jasper. Rocks of andesitic affinity are abundant in this group within the northern half of the IPB domain. The youngest unit is the Carboniferous CG, which is a thick turbiditic sequence of shale, greywacke and conglomerate.

The SPZ has evidences of major magmatism, which is represented by the volcanic rocks of the VSC (Munhá, 1983; Mitjavila *et al.*, 1997) and the plutonic rocks of the SNB (*e.g.* Simancas, 1981; Schütz *et al.*, 1987; de la Rosa, 1992; Díez-Montes and Bellido Mulas, 2008). The SNB intrudes Devonian rocks of PQG and has complex relationships with the volcanic rocks of

the VSC, due to the subvolcanic nature of some of the intrusions (Simancas, 1983). Two main intrusive suites make the Sierra Norte Batholith. Gabbros and diorites, with associated ultramafic cumulates, constitute the first suite. The second suite, and the one with largest areal extension, is a set of subvolcanic intrusions of tonalite, trondhjemite and granodiorite. The age of these intrusions range from 356 to 330Ma (Kramm *et al.*, 1991; Barrie *et al.*, 2002; Dunning *et al.*, 2002; Braid *et al.*, 2012). A small separate set of discrete peraluminous, S-type granitoids known as El Berrocal and Navahonda granites (de la Rosa *et al.*, 1993) and the El Crispinejo granite (Díez-Montes and Bellido Mulas, 2008) constitute the last intrusive pulse of the SPZ. The Berrocal granite has a reported Rb-Sr age of 300 ± 6Ma (Quesada *et al.*, 1989). The Berrocal granite intrudes Lower Carboniferous strata and is locally overlaid by the sediments and volcanic rocks of the late Stephanian-Autunian El Viar basin, while

the Navahonda and Crispinejo granites also intrude the TTG suite of the Sierra Norte Batholith.

El Crispinejo granite

The El Crispinejo granite is located to the northwest of the village of Minas del Castillo de las Guardas (province of Seville). It is a small (*ca.* 2km^2) plutonic body of porphyritic granite, which intrudes the granitoids of the TTG series of the Sierra Norte Batholith (Figs. 1 and 2). Weathering of the granite results in a topographic low, which is crossed by El Crispinejo stream. The granite crops out quite well in the vicinity of the stream (Fig. 3), forming metric boulders with subangular shapes due to a well-developed joint system. When fresh, the rock has a white to light grey colour, and ranges from medium-coarse (5-7mm) to medium (2-5mm) grain size. The medium-size facies occupy the northern portion of the pluton, near the intersection of the El Crispinejo and La Siguereja stream, while the coarser facies are observed in the southern portion of the intrusion. The porphyritic character of the intrusion is given by the presence of dispersed, tabular (2-4cm x 1cm), K-feldspar megacrystals with a 10-20cm^2 spacing between them (Fig. 3). The two-micas granitic groundmass range from medium-coarse (5-7mm) to medium (2-5mm) grain size. A very distinctive character of this intrusion is the presence of cordierite prisms up to 10mm in length (Fig. 3D), which is quite unique among intrusion of the SPZ. The facies with medium-size groundmass occupies the northern portion of the pluton, near the intersection of the El Crispinejo and La Siguereja stream, while the coarser facies are observed in the southern portion of the intrusion.

Along its southern border (Fig. 2), the granite intrudes rocks of the VSC, generating contact metamorphism (Fig. 4). Cordierite blasts are produced in the pelitic members of the surrounding VSC. The granite also cuts minor folds in the VSC suggesting that it is a late intrusion.

The granite is associated with two separate ore showings (García-Cortés, 2011). The most significant one is the "Los Angeles" mine, a F-Pb-Zn prospect formed by quartz veins filling a fault gauge with 0.5 to 1.5 meters thick, and up to 2km long. The other prospect is located within the granite, near its southern boundary with the rocks of the VSC. It consists of a set of 15 to 45cm thick and 6 to 8 meters long veins with Sn-W mineralization.

Petrography

The El Crispinejo granite presents a porphyritic hipidiomorphic texture. The megacrystals are of tabular K-feldspar (2-4cm x 1cm). The groundmass ranges from medium-coarse (5-7mm) to medium (2-5mm) grain size. The major minerals are quartz (40-45%), K-feldspar (30-35%), plagioclase (15-20%), biotite (3%) and muscovite (2%). Cordierite is also present but in smaller proportion (<1%). Zircon, monazite, apatite, tourmaline and opaques occur as accessory minerals. Secondary minerals include chlorite, titanite, K-feldspar, ilmenite, biotite, muscovite, pinnite, sericite, sagenitic rutile, calcite and epidote.

The quartz crystals generally have anhedral to hypidiomorphic rounded shapes, with occasionally well-developed crystal faces; some have round embayments. The crystals are monocrystalline or display irregular subgrains with normal and ondulose extinction, and exhibit biotite and plagioclase inclusions. Occasionally, rounded quartz can be up to 7-10mm in diameter.
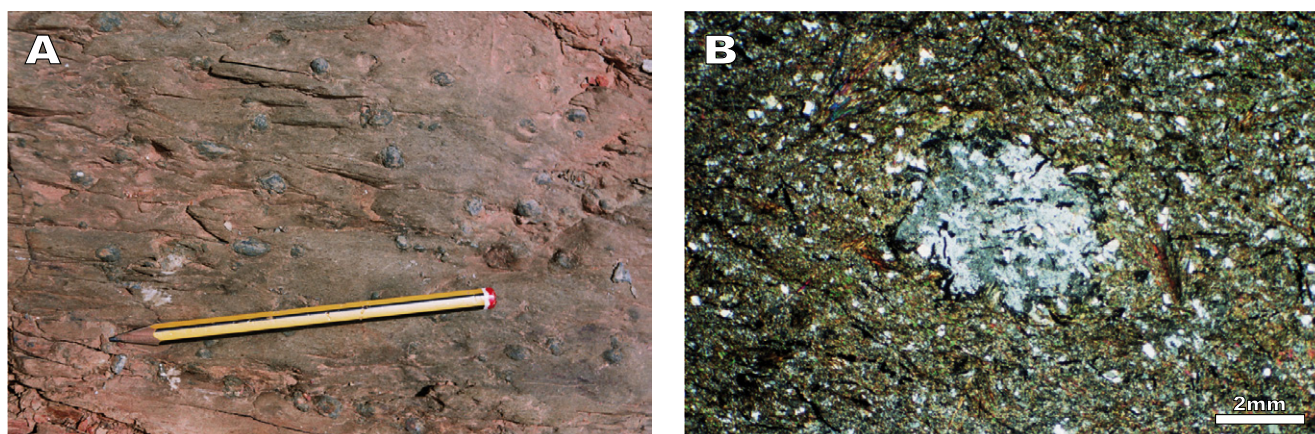

FIGURE 4. Contact metamorphism of the El Crispinejo granite. A) Blasthesis of cordierite in pelitic lithologies of the Vulcano-Sedimentary Complex (VSC). B) Microphotograph of a cordierite blast.
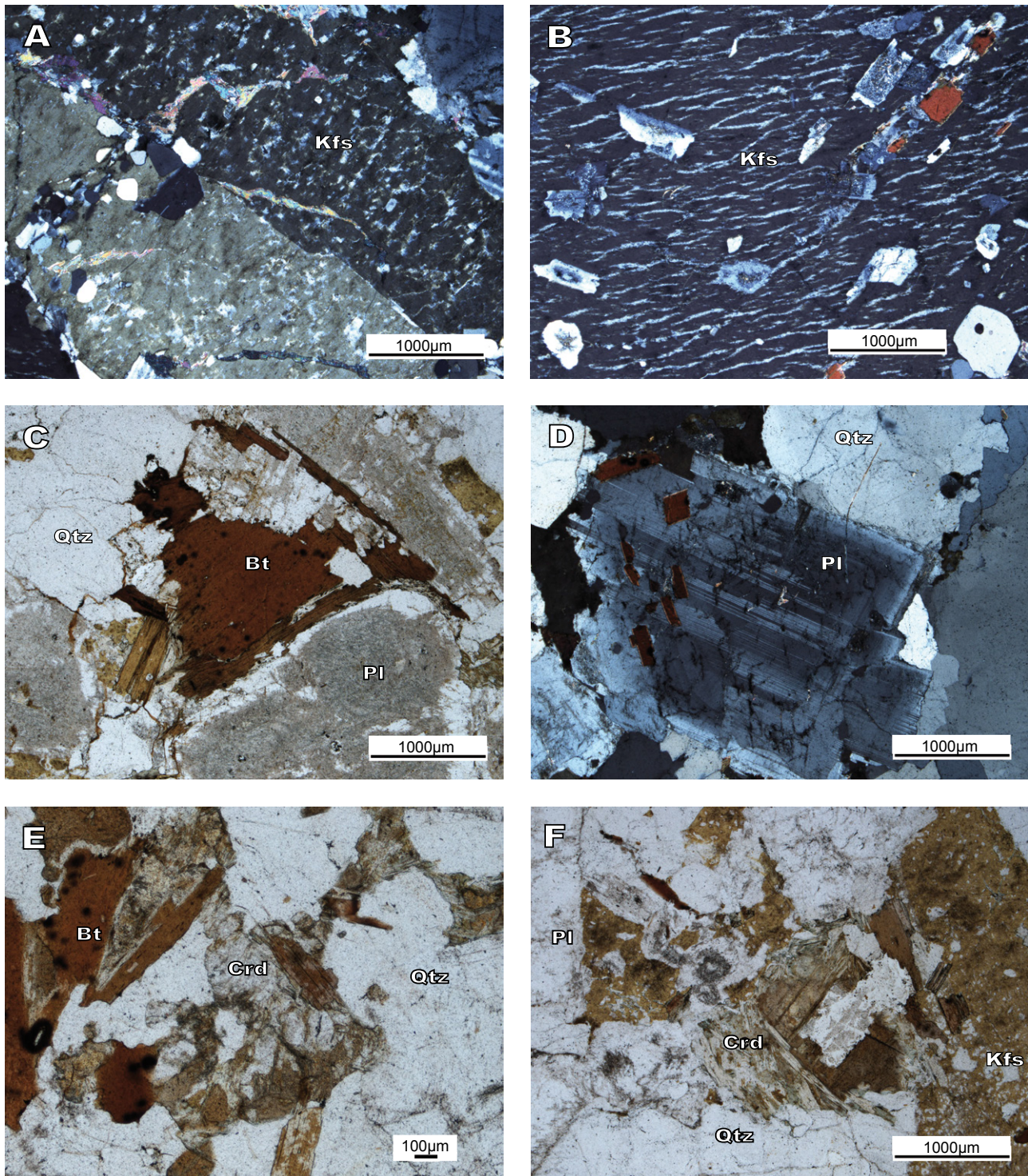
FIGURE 5. Microtextures of the El Crispinejo granite. A) K-feldspar phenocryst with Carlsbad twin, film-type perthites and quartz inclusions. The cracks of the phenocryst are filled with white mica. B) Detail of film-type perthites and plagioclase, biotite, quartz inclusions defining a Frasl texture in a K-feldspar megacryst. C) Textural aspect of the granite with plagioclase partially retrogressed to sericite. D) Plagioclase crystal with polysynthetic twin and a weak concentric zonation. Biotite inclusions are disposed parallel to the concentric zonation. E) Cordierite crystal (center) with a fresh core and a retrogressed rim. F) Prismatic section of a cordierite crystal completely retrogressed to a mica aggregate. (Qtz: quartz; Bt: biotite; Kfs: potassic feldspar; Pl: plagioclase; Crd: cordierite).

The K-feldspar crystals occur as large megacrystals and in the groundmass of the porphyritic granite. They display tabular hypidiomorphic shapes with microcline and Carlsbad twins (Fig. 5A), and "film" and "vein" perthitic textures. The K-feldspars are rich in inclusions of quartz, biotite and plagioclase. These inclusions are often disposed parallel to the borders of the megacrysts (Fig. 5B). Where the K-feldspar crystals are in contact with each other, there is intergranular, polycrystalline, plagioclase in interstitial position. The plagioclase crystals are hypidiomorphic showing polysynthetic twins and occasional concentric zoning (Fig. 5D). When zoned, the core of the plagioclase crystals is retrogressed to a very fined grained aggregate of sericite, epidote and calcite. Biotite is present in the groundmass as forming aggregates of 3 to 6 crystals. It has a hypidiomorphic shape with reddish brown to yellow brown pleochroism (Fig. 5C), and displays zircon and monazite inclusions. The biotite is variably altered and transformed by chloritization. Muscovite occurs in the groundmass as euhedral crystals, suggesting a primary origin. It also occurs as anhedral crystals with biotite inclusions and as anhedral inclusions in the twins and exfoliation planes of K-feldspar, indicating a secondary origin. Although, not a major mineral, cordierite can be observed as hypidiomorphic and euhedral prims up to 10mm in length (Fig 5E). Often it is retrogressed, but fresh crystals are also preserved. When retrogressed cordierite is transformed by pinnitization or transformed to a mica aggregate (muscovite+biotite+chlorite) (Fig.5F).

Geochemistry

Major and trace element analyses were done in five representative samples from El Crispinejo granite (Table 1). This also includes samples AD9035 and AD9036 from Díez-Montes *et al.* (1999). For comparison purposes, in order to show the difference between this granite and surrounding granitoids of the Sierra Norte Batholith, samples from the country rock trondhjemitic granitoids are displayed in the diagrams, these data are from Díez-Montes *et al.* (1999). All the analyses, including sample preparation, were done at the IGME laboratories. Major elements were done by XRF and AAS (Na). The trace element analyses were done by XRF on press-pellets using pro-trace software, while the REE´s were done by ICPMS on fused pellets.

This granite has a high but narrow range of SiO_2 content (73.64-75.28%; Fig. 6). The sample shows a very small compositional variation with low CaO, $Fe_2O_3^t$ and MgO values. According to the major element classification scheme of Middlemost (1994; Fig. 6), the samples plots in the granite field. The cordierite-

bearing El Crispinejo granite has the classic mineralogy of S-type peraluminous granites (Chappell and White, 1974). The peraluminous character is confirmed by an alumina saturation index (ASI) between 1.1 and 1.3, and the presence of normative corundum (1.5-2.8).

The granite has a moderately fractionated chondrite-normalized REE pattern (Fig. 7A; La/Yb_N=5.9-9.18), with an enrichment in LREE (La/Sm_N= 3.52-3.96), a negative Eu anomaly (Eu/Eu*=0.37-0.67) and almost flat

TABLE 1. Geochemical data for the El Crispinejo granite (IGME laboratories)

| SAMPLE	939-1	939-2	939-3	AD9035	AD9036
UTM Coordinates. System ED50. 29S					
Coord. X	731.115	730.562	731.129	731200	730.270
Coord. Y	4.176.513	4.177.389	4.176.660	4.176.640	4.177.760
SiO_2	74.95	73.61	73.04	73.58	73.30
TiO_2	0.18	0.27	0.20	0.18	0.14
Al_2O_3	13.60	14.24	14.64	13.80	14.15
$Fe_2O_3^t$	1.64	2.15	1.86	1.52	1.18
MnO	0.06	0.05	0.06	0.05	0.05
MgO	0.50	0.50	0.50	0.33	0.31
CaO	1.10	1.23	0.82	1.12	0.85
Na_2O	3.23	3.40	3.46	3.42	3.58
K_2O	4.41	3.56	4.69	4.48	4.26
P_2O_5	0.10	0.10	0.10	0.10	0.13
LOI	0.55	1.00	0.86	0.67	0.91
TOTAL	100.31	100.11	100.23	99.25	98.86
Sc	4.8	5.2	5.3	5	4
V	7.8	14.6	9.2	5	7
Cr	0	0	0	17	10
Co	0	0	0	1.2	1
Ni	0	0	1.5	19	18
Cu	0	0	0	0	16
Zn	16.2	20.5	24.9	42	32
Ga	18.5	21.2	20.5	23	20
As	4.7	11.9	5.4	7	57
Rb	252.6	240.8	280.6	308	243
Sr	100.6	131.2	95.1	115	125
Y	23.3	28.1	25.5	27	22
Zr	93.1	126	110.4	109	65
Nb	10.9	12.4	12.2	12	8.9
Mo	0	0	0	4	0.4
Ag	0	0	0	0.7	0.5
Sn	5	6.6	5.1	7.7	10
Sb	0	0	0	0.32	0.17
Cs	15.9	23.5	14.7	18	17
Ta	0	0	3.1	2.46	1.93
Ba	293.3	228.8	316.2	379	300
La	27.9	33	33.7	30.8	18
Ce	57.2	68.5	69.7	61.8	36.5
Pr	6.52	7.9	7.99	6.9	3.74
Nd	23.5	28.3	28.6	28.2	15.3
Sm	4.86	5.77	6.03	4.9	3.17
Eu	0.66	0.79	0.66	0.603	0.672
Gd	4.38	5.2	4.97	5.09	3.05
Tb	0.7	0.82	0.8	0.84	0.57
Dy	4.31	5.08	4.75	4.29	3.38
Ho	0.83	0.98	0.88	0.82	0.68
Er	2.41	2.99	2.7	2.79	1.98
Tm	0.36	0.42	0.4	0.438	0.318
Yb	2.53	2.86	2.48	2.58	2.06
Lu	0.36	0.4	0.35	0.38	0.301
Hf	0	0	0	3.9	2.3
W	0	0	3	1.1	34
Tl	0	0	2.8	2.26	1.57
Pb	38.6	34	40.2	65	64
Th	16.1	17.8	19.7	17.7	9.11
U	0	6.7	6.2	10.1	7.61
Ge	2.1	2.2	2	2.3	2.3
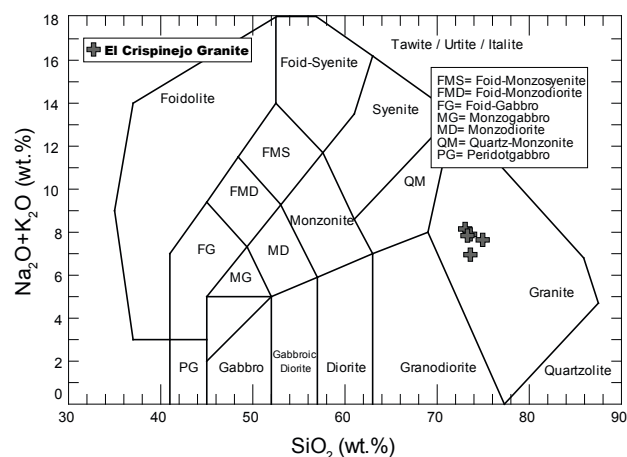
FIGURE 6. TAS diagram by Middlemost (1994).

HREE (Gd/Yb_N=1.2-1.6). When normalized to "Primitive mantle" (Sun and McDonough, 1989; Fig. 7B), the pattern shows significant negative anomalies in Ba, Nb, Sr, Eu and Ti, that could be attributed to fractionation of plagioclase, K-feldspar and biotite, and positive anomalies in Th and U.

The El Crispinejo granite is, therefore, enriched in K_2O, Rb, Th and Ta, and has average to low values of Zr, Hf, Sm, Y, Yb and Sr and a peraluminous character typical of collisional granites (Pearce *et al.*, 1984; Harris *et al.*, 1986; Pearce, 1996a). The granite tectonic discrimination diagrams of Pearce *et al.* (1984, 1996b; Fig. 8) show that while the trondhjemitic granitoids of the SNB plot at the boundary of the volcanic arc (VAG), within-plate and ocean-ridge (ORG) granite field, the El Crispinejo granite plots in a separate position at the boundary of the syn-collisional –VAG field. This position is typical of collisional granites (Pearce *et al.*, 1984; Pearce, 1996b), as confirmed by the Rb-Hf-Ta diagram of Harris *et al.* (1986; Fig.8C). In the Nb/Ta-Zr/Hf diagram of Ballouard *et al.* (2016; Fig. 8D)

the granite plots in the field of the Sn-W mineralized granites. So, the geochemistry of the granite confirms the field and petrographic observations that conclude that it is late- to post-collisional, peraluminous, S-type granite with associated Sn-W mineralization.

Geophysical data

The radiometric data is part of a geophysical flight done in the Iberian Pyrite Belt between November 1996 and April 1997 with a spacing of 250 meters and a nominal height of 80 meters. These data are available from the Geophysical Information System of IGME (SIGEOF; http://info.igme.es/sigeof/). The lines corresponding to the %K, ppm Th and ppm U were processed at the unit of geophysics and remote sensing of IGME. The images of the potassium concentration and the ternary (combination of U, Th and K) do provide a strong contrasting signal with the surrounding country rock. The image of the potassium concentration shows a clear positive anomaly with values over 6% that match the outline of the granite mapped in the field (Fig. 9). Along the northern boundary, the anomaly goes beyond the mapped area suggesting that the granite extents a little bit further up. On the southeastern corner of the granite, the anomaly is weak due to the fault contact between the granite and gabbro-diorite with a lower radiometric response. The central part of the granite also shows strong Th (>21ppm) and U (>5ppm) positive anomalies (Figs. 9B and C). The same type of geophysical anomalies has been observed in the Berrocal granite (Bellido *et al.*, 2006), a similar S-type peraluminous granite located in the NE sector of SPZ.

U-PB ID-TIMS GEOCHRONOLOGY

A sample was collected from the central part of the El Crispinejo granite for U-Pb dating (star in Fig. 2).

TABLE 2. U-Pb geochronological data, El Crispinejo granite

Fractions	Weight (mg)	U (ppm)	Pb (ppm)	Pb (pg)	$\frac{^{206}Pb^*}{^{204}Pb}$	$\frac{^{208}Pb}{^{206}Pb}$	$\frac{^{206}Pb}{^{238}U}$	% err	$\frac{^{207}Pb}{^{235}U}$	% err	$\frac{^{207}Pb}{^{206}Pb}$	% err	$\frac{^{206}Pb}{^{238}U}$	$\frac{^{207}Pb}{^{235}U}$	$\frac{^{207}Pb}{^{206}Pb}$	*Rho*
4009-4																
M1(6 Mnz xtals)	0.0034	5425	1962	411	136.5	7.083	0.04772	0.21	0.3445	0.67	0.05236	0.62	300.5	300.6	301.3	*0.37*
M2 (6 Mnz xtals)	0.0034	6552	1548	198	315.6	4.424	0.04771	0.21	0.3445	0.26	0.05234	0.26	300.4	300.4	300.2	*0,81*
M3 (7 Mnz xtals)	0.0040	5508	1708	187	288.9	6.278	0.047096	0.60	0.3412	4.23	0.05254	3.94	296.7	298.1	309.0	*0.54*
Z1 (5 small Zrn prisms)	0.0040	311	39	101	55.0	0.089	0.047439	1.24	0.3424	2.61	0.05236	2.20	298.8	299.0	301.0	*0.55*
Z2 (2 large+3 small Zrn)	0.0050	344	16	28	195.5	0.124	0.045896	1.22	0.3301	2.35	0.05217	1.93	289.3	289.7	292.9	*0.57*
Z3 (8 small Zrn prisms)	0.0060	294	15	5	957.5	0.202	0.047162	0.65	0.3408	0.93	0.05241	0.64	297.1	297.8	303.4	*0.71*

M (Mnz): monazite; Z (Zrn): zircon. Large (*ca.*100μm long), small (*ca.*50μm long) Number of crystals (xtals) in each fraction is given within brackets. Pb (pg), total common Pb blank. *Measured ratio corrected for blank and fractionation. Atomic ratios corrected for fractionation (0.11±0.02% AMU Pb; 0.10±0.02% AMU, U), monazite spike (^{208}Pb-^{235}U), zircon spike (BSU-1B spike, ^{205}Pb-^{233}U-^{235}U, courtesy MIT lab), laboratory blanks (6pg Pb; 0.1pg U) and initial common Pb after Stacey & Kramers (1975). Errors are at the 2-sigma level. Data reduced with PbMacDat (Isachsen *et al.*, www.earth-time.org).

The sample was processed and dated using the U-Pb ID-TIMS method at IGME laboratories. Monazite and zircon were selected for analyses after rock crushing and mineral separation, dissolved, and the U and Pb chemically separated using the techniques described in Valverde-Vaquero (2009). For monazite isotope dilution (ID) analysis a ^{208}Pb-^{235}U spike was used; while for zircon analysis a ^{205}Pb-^{233}U-^{235}U spike (spike BSU-1B, courtesy of the MIT laboratory) was used. In case of zircon, the crystals were pretreated with the chemical abrasion method of Mattison (2005) before dissolution. Isotopic relationships were measured with a Triton multicollector TIMS mass spectrometer equipped with an axial secondary multiplier ion counter. Pb was measured in the 1300-1500°C temperature range and uranium was measured as dioxide at temperatures between 1450-1600°C (for further details see Rubio Ordoñez *et al.*, 2012). The artificial Earthtime 500Ma solution was used to test the calibration of both spikes and the oxide correction in the case of uranium measurements with the triple spike, assuring accuracy within 0.1% in all cases. The data was processed using the Pb MacDat spreadsheet of Isachen *et al.* (2007). All reported isotopic ratios are corrected for mass fractionation (Pb 0.11±0.02% AMU, U 0.10±0.02%), blank (2-5pg Pb, 0.1pg U) and initial common Pb. U-Pb diagrams and age calculations were done with ISOPLOT (Ludwig, 1999).

A total of three monazite and three zircon fractions were analyzed (Table 2). All fractions are concordant to subconcordant, overlapping the Concordia curve between 300 and 290Ma (Fig. 10). The six fractions define a Discordia line with an upper intercept age of 300±3Ma. This upper intercept age is anchored by two concordant monazite fractions with a "Concordia age" of 300.5±0.5Ma (Fig. 10). The other monazite fraction, which had measurement problems during mass spectrometry, is slightly discordant. The zircon fractions are also slightly discordant, suggesting that minor secondary Pb-loss was still present, despite the chemical abrasion. Fractions Z1 and Z3 are collinear with the Discordia line, fraction Z2 is slightly off to the left but within error. Considering the whole data set, the two concordant monazite fractions with an age of 300.5±0.5Ma provide the best age estimate. However, in order to avoid underestimating the error, we prefer to expand the lower error to include an overlap with the centroid of zircon fraction Z1, and quote an age of 300.5+0.5/-1.5Ma as our most accurate estimate for the age of granite intrusion.

DISCUSSION

The new data on the El Crispinejo granite indicates the presence of a distinctive peraluminous, S-type,

granite suite of Permo-Carboniferous age in the SPZ. The 300Ma U-Pb age of El Crispinejo confirms a reported Rb-Sr age 300±6Ma for El Berrocal granite (Quesada *et al.*, 1989) This suggests that in addition to El Crispinejo, this granite suite includes the Navahonda and Berrocal garnet-bearing monzogranites of De la Rosa *et al.* (1993). As shown by De la Rosa *et al.* (1993), these granites have high ($^{87}Sr/^{86}Sr_{(300Ma)}$) signatures (0.718 to 0.729) very different from the 330-350Ma granitoid suites of the Sierra Norte Batholith (0.703 to 0.708). The Crispinejo granite shows Nb/Ta and Zr/Hf ratios that coincide with those of the peraluminous granites associated with Sn-W mineralization, which is consistent with the Sn-W ore prospect associated with this granite.

The El Crispinejo-Berrocal-Navahonda peraluminous granite suite resembles some of the Sn-W mineralized peraluminous granites of the Central Iberian Zone (CIZ). For example, some peraluminous granites of the Central
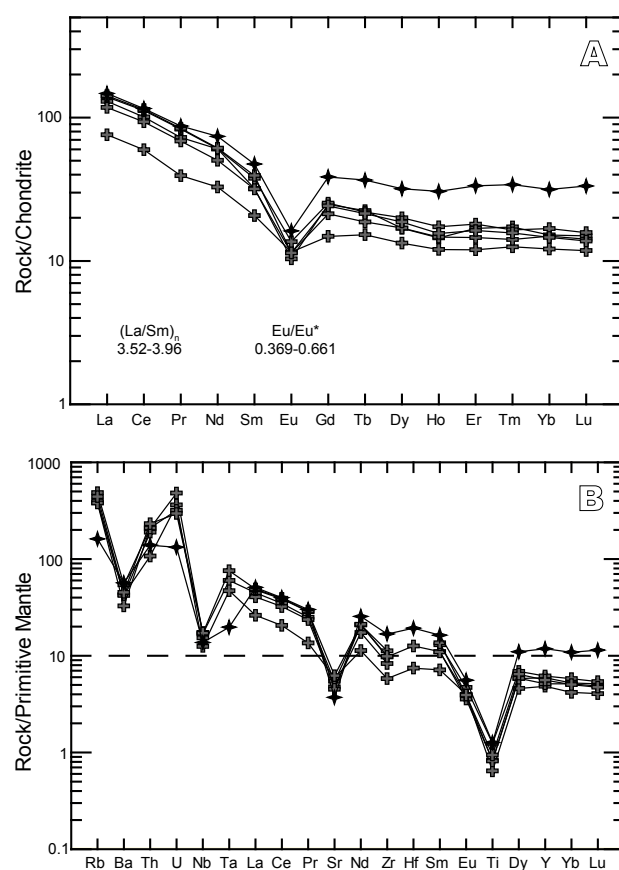

FIGURE 7. Multi-element diagrams showing the comparison between the El Crispinejo granite and the trondhjemitic granites of the SPZ. A) Chondrite-normalized Rare Earth element pattern. B) Primitive mantle-normalized trace element pattern. The crosses represent samples from the El Crispinejo granite. The four-point start pattern represents an average value of the trondhjemitic granite of the SPZ. Normalizing values after Sun and McDonough (1989).
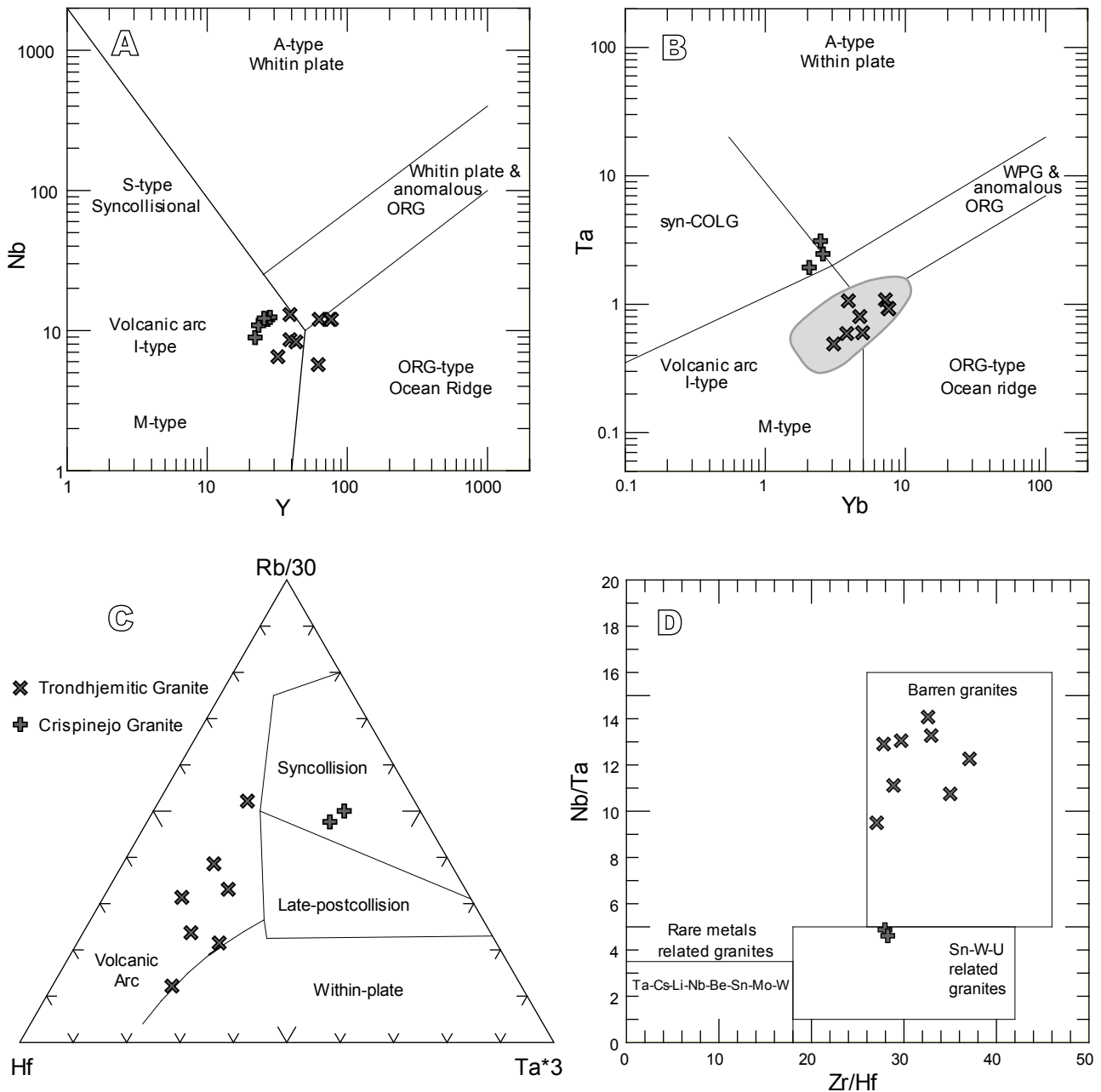
FIGURE 8. Geochemical tectonic discrimination diagrams. A, B) Tectonic diagrams of Pearce *et al.* (1984), in grey the field of trondhjemitic granites of the SPZ. C) Tectonic discrimination diagram of Harris *et al.* (1986). D) Nb/Ta *vs.* Zr/Hf diagram from Ballouard *et al.* (2016).

Extremadura Batholith, like the Logrosan granite, have a highly radiogenic initial Sr isotopic signature ($^{87}Sr/^{86}Sr_{(300Ma)}$ 0.7125-0.7286; *e.g.*, Sr data in Chicharro *et al.*, 2014). It should be noted that in the CIZ the Sn-W mineralization occurs both in S-type and I-type granites, although these latter granites show less radiogenic Sr signatures (see Neiva, 2002). It is generally accepted that these peraluminous granites are derived from partial melting of crustal metasedimentary sources similar to the Neoproterozoic Schistose Greywacke Complex (*e.g.*

Villaseca *et al.*, 2008). Late Variscan, tin-mineralized, peraluminous granites are also abundant in SW England, an area which is considered the classic continuation of the SPZ along the European Variscides (*e.g.* Franke, 1992). The S-type granites of the Cornubian Batholith exhibit high initial Sr isotopic ratios. According to Chappell and Hine (2006), the Cornubian granites, like their Central Iberian counterparts, were derived from partial melting of feldspathic greywackes. In the SPZ, feldspathic greywackes occur at the base of the eastern

end Phyllite-Quartzite Group (Fig. 1) in the Lower Devonian La Minilla Fm. (Simancas, 1983). These rocks present the highest metamorphic grade of the SPZ (garnet-zone), and they could be a potential source for these S-type granites.

Bea (2012) provides a clear outline of the different mechanisms and sources of heat involved in granite genesis. These concepts can be used to make some inferences regarding the genesis of the El Crispinejo granite suite. The El Crispinejo granite is enriched in the three heat producing elements (HPE; U, Th, and K), which produce its contrasting radiometric geophysical signature. According to Bea (2012), "*granites contain*

the same or lower HPE as their sources". This characteristic would imply that the El Crispinejo granite was derived from melting a crustal source originally enriched in heat producing elements. Such a source would be consistent with a feldspathic greywacke source, as that proposed by Chappell and Hine (2006) for the Cornubian S-type granites of SW England. This crustal source however, does not appear to have been tapped by the previous 330-350Ma magmatic events in the SPZ. In contrast to the batholiths of SW England, the S-type granites of the SPZ are small bodies, which suggests that crustal melting was limited in areal extent. The 300.5 +0.5/-1.5Ma age of El Crispinejo granite is broadly contemporaneous with the opening of the
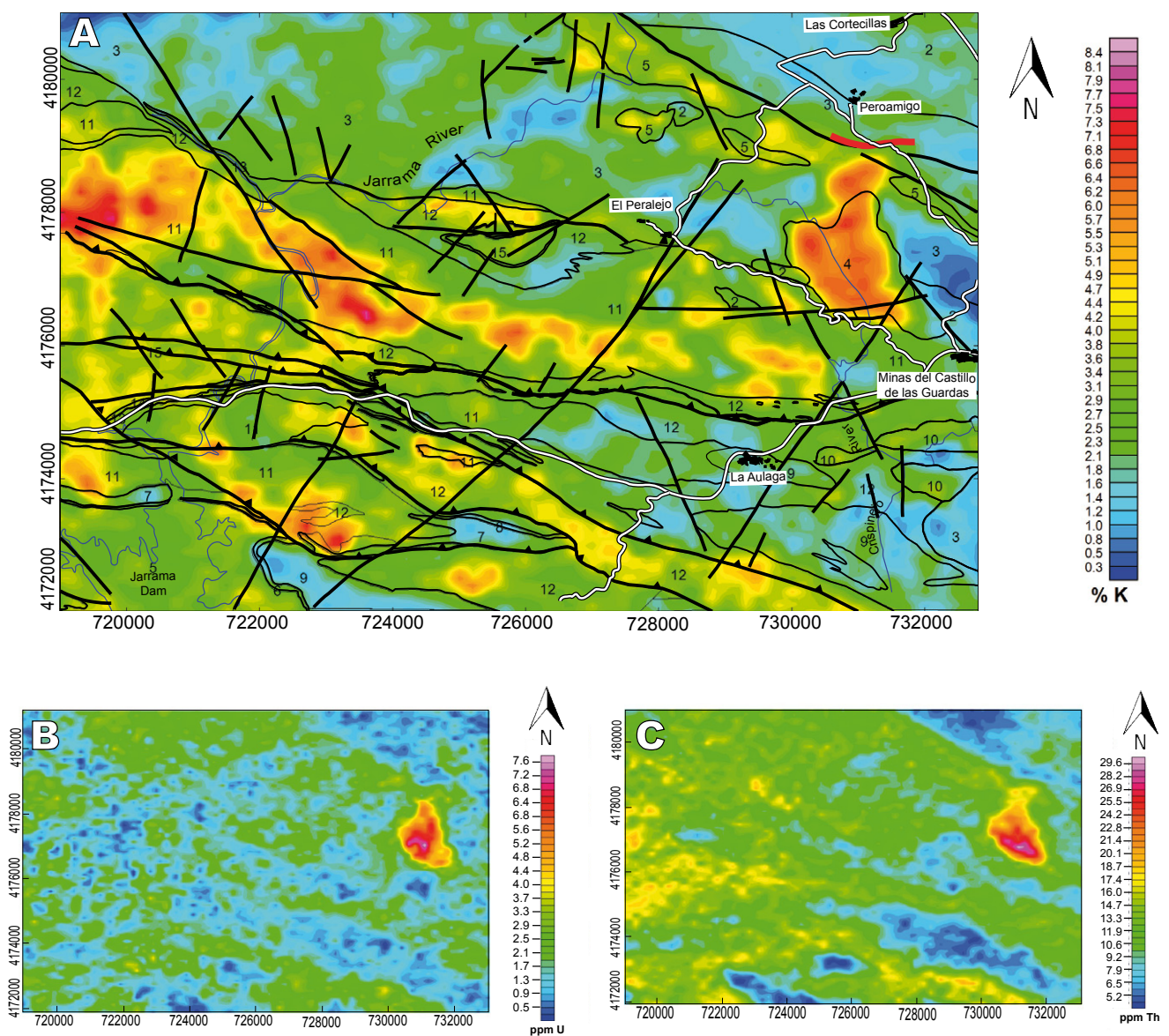

FIGURE 9. Geophysical radiometric anomalies around the El Crispinejo granite. A) Potassium (K) radiometric anomaly. B) Uranium radiometric anomaly. C) Thorium radiometric anomaly.
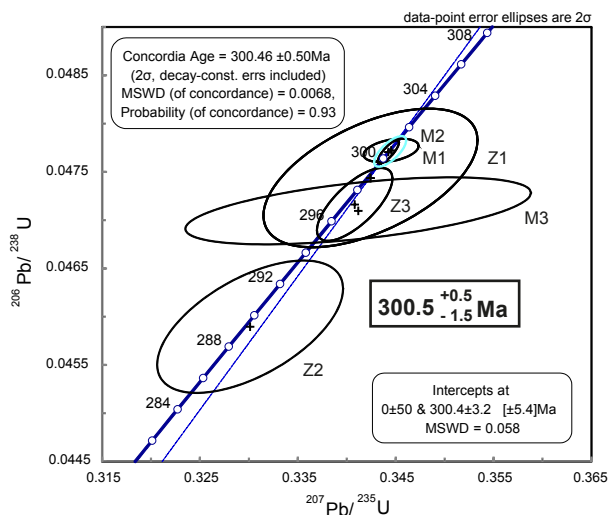
FIGURE 10. U-Pb Concordia diagram for El Crispinejo granite. Z, zircon; M, monazite. U-Pb ID-TIMS data (Table 2).

El Viar Basin during the Permo-Carboniferous. This basin contains strata with Stephanian-Autunian flora intercalated with basaltic lava flows (*e.g.* Simancas, 1981). The peraluminous Berrocal granite occupies one of the flanks of the basin and conglomerates with clasts of this granite have been described in the basin. This evidence suggests a close spatial and temporal relationship between the S-type granite intrusions and the onset of the Permo-Carboniferous volcanism. The intrusion and crystallization of mantle-derived magmas in the crust, intraplatting, is one of the most effective forms of heat transfer (Bea, 2012) and would trigger local anatexis producing granitic melts. We speculate that these discrete peraluminous granites might have been produced by local heat transfer from the Permo-Carboniferous mantle-derived magmas, inducing local anatexis of a fertile greywacke source at middle or upper crustal levels.

CONCLUSIONS

The cordierite-bearing El Crispinejo granite forms part of a distinctive suite of peraluminous S-type granites that intrude the Volcano-Sedimentary Complex and the TTG granitoid suite of the Sierra Norte Batholith. These granites have a remarkable, contrasting, radiometric geophysical signature due to their K-enrichment. The geochemistry of El Crispinejo granite is similar to that of mineralized Sn-W peraluminous granites, which is consistent with the presence of Sn-W mineralization associated with the granite. The U-Pb dating of monazite and zircon provides an age of 300.5 +0.5/-1.5Ma, which indicates that these granites are associated with a Permo-Carboniferous magmatic pulse, coeval in time with the

extrusion of Late Stephanian-Autunian basalts in the nearby El Viar basin.

ACKNOWLEDGMENTS

REFERENCES

Ballouard., C., Poujol, M., Boulvais, P., Branquet, Y., Tartèse, R., Vigneresse, J.L., 2016. Nb-Ta fractionation in peraluminous granites: A marker of the magmatic-hydrothermal transition. Geology, 44 (3), 231-234.

Barrie, C.T., Amelin, Y., Pascual, E., 2002. U-Pb geochronology of the VMS mineralization in the Iberian Pyrite Belt. Mineralium Deposita, 37, 684-703.

Bea, F., 2012. The sources of energy for crustal melting and the geochemistry of heat-producing elements. Lithos, 153, 278-291.

Bellido, F., Díez-Montes, A., Ortiz, G., 2006. Estudio petrológico y geoquímico de las vulcanitas de los afloramientos de El Pimpollar, extremo nororiental de la Zona Surportuguesa. Geogaceta, 40, 127-130.

Braid, J.A., Brendan Murphy, J., Quesada, C., Bickerton, L., Mortensen, J.K., 2012. Probing the composition of unexposed basement, South Portuguese Zone, southern Iberia: implications for the connections between the Appalachian and Variscan orogens. Canadian Journal of Earth Sciences, 49, 591-613.

Chappell, B.W., White, A.J.R., 1974. Two contrasting granites types. Pacific Geology, 8, 173-174.

Chappell, B.W., Hine, R., 2006. The Cornubian Batholith: an Example of Magmatic Fractionation on a Crustal Scale. Resource Geology, 56(3), 203-244.

Chicharro, E., Villaseca, C., Valverde-Vaquero, P. Belousova, E., López-García, J.A., 2014. Zircon U-Pb and Hf isotopic constraints on the genesis of a post-kinematic S-type Variscan tin granite: the Logrosán cupola (Central Iberian Zone). Journal of Iberian Geology, 40(3), 451-470.

de la Rosa, J.D., 1992. Petrología de las rocas básicas y granitoides del batolito de la Sierra Norte de Sevilla, Zona Surportuguesa, Macizo Ibérico. Doctoral Thesis, Universidad de Sevilla, 312pp.

de la Rosa, J.D., Rogers, G., Castro, A., 1993. Relaciones [87]Sr/[86]Sr de rocas básicas y granitoides del Batolito de la Sierra Norte de Sevilla. Revista de la Sociedad Geológica de España, 6(1-2), 141-149.

Díez-Montes, A., Bellido Mulas, F., 2008. Magmatismo TTG y Al-K en la Zona Surportuguesa. Relaciones entre plutonismo y vulcanismo. Geo-Temas, 10, 1449-1452.

Díez-Montes, A., Leyva, F., Matas, J., Martín Parra, L.M., 1999. Mapa Geológico a escala 1:50.000 y Memoria de El Castillo de las Guardas (939). Investigación Geológica y Cartografía Básica en la Faja Pirítica y Áreas Aledañas. Available on line at: www.juntadeandalucia.es/ economiainnnovacioncienciayempleo/pam.

Dunning, G.R., Díez-Montes, A., Matas, J., Martín Parra, L.M., Almarza, J., Donaire, M., 2002. Geocronología U/Pb del volcanismo ácido y granitoides de la Faja Pirítica Ibérica, Zona Surportuguesa. Geogaceta, 32, 127-130.

Franke, W., 1992. Phanerozoic structures and events in Central Europe. In: Blundell, D., Freeman, R., Mueller St. (eds.). A continental rrevealed: the European Geotraverse. Cambridge University Press, Cambridge, 164-179.

García-Cortés, A. (ed.). 2011. Cartografía de recursos minerales de Andalucía. IGME-Consejería de Economía, Innovación y Ciencia de la Junta de Andalucía, Madrid, 608pp.

Harris, N.B.W., Pearce, J.A., Tindle, A.G., 1986. Geochemical characteristics of collision-zone magmatism. In: Coward, M.P., Alison, C. (eds.). Collision Tectonics. Geological Society London Special Publications, 19, 67-81.

IGME, Instituto Geológico y Minero de España, 1994. Mapa Geológico de la Península Ibérica, Baleares y Canarias. 1:50.000. Madrid, Servicio de Publicaciones del Instituto Geológico y Minero de España. Available at: http://info. igme.es/sigeof/

Isachen, C.E., Coleman, D.S., Schmitz, M., 2007. Pb MacDat program, Available at http://www.earthtime.org (last access: 2015).

Kramm, U., Giese, D., Zhuravlev, D., Walter, R., 1991. Isotope equilibration of magmatism and metamorphic rocks of the Aracena Metamorphic Belt. In: XI Reunión sobre la Geología del Oeste Peninsular, Universidad de Sevilla, Huelva, España.

Lotze, F., 1945. Zur Gliederung der Varisciden der Iberischen Meseta. Geotektonik Forschung, 6, 78-92. (Translated into Spanish by Ríos, J. M., 1950: Observaciones respecto a la división de las varíscides de la Meseta Ibérica. Publicaciones Extraordinarias de la Geología de España, V, 149-166).

Ludwig, K.R., 1999. ISOPLOT/Ex. version 2.00: A Geochronological Toolkit for Microsoft Excel. Berkeley Geochronology Center, Special Publication, 1a, 46pp.

Mattison, J.M., 2005. Zircon U-Pb chemical abrasion ("CA-TIMS") method: Combined annealing and multistep partial dissolution analysis for improved precision and accuracy of zircon ages. Chemical Geology, 220, 47-66.

Middlemost, E.A.K., 1994. Naming materials in the magma / igneous rocks system. Earth-Science Reviews, 37, 215-224.

Mitjavila, J., Martí, J., Soriano, C., 1997. Magmatic evolution and tectonic setting of the Iberian Pyrite Belt Volcanism. Journal of Petrology, 38, 727-755.

Munhá, J., 1983. Hercinian magmatism in the Iberian Pyrite Belt. In: Lemos de Souza, J., Oliveira, J.T. (eds.). The Carboniferous of Portugal. Memórias do Serviço Geológico de Portugal, 29, 39-81.

Neiva, A.M.R., 2002. Portuguese granites associated with Sn-W and Au mineralizations. Bulletin of the Geological Society of Finland 74, Parts 1-2, 79-101.

Oliveira, J.T., 1990. South Portuguese Zone: Stratigraphy and Synsedimentary Tectonism. In: Dallmeyer, R.D., Martínez García, E. (eds.). Pre-Mesozoic Geology of Iberia. Springer-Verlag, Berlin, 333-347.

Oliveira, J.T., Horn, M., Paproth, E., 1979. Preliminary note on the stratigraphy of the Baixo Alentejo Flysh Group, Carboniferous of Portugal, and on the paleogeographic development to corresponding units in northwest Germany. Comunicações do Serviço Geológico de Portugal, 65, 151-168.

Pearce, J.A., 1996a. A User's Guide to Basalt Discrimination Diagrams. In: Wyman, D.A. (ed.). Trace Element Geochemistry of Volcanic Rocks: Applications for Massive Sulphide Exploration. Geological Association of Canada, Short Course Notes, Vol. 12, 79-113.

Pearce, J.A., 1996b. Sources and setting of granitic rocks. Episodes, 19 (4), 120-125.

Pearce, J.A., Harris, N.B., Tindle, A.G., 1984. Trace element discrimination for the tectonic interpretation of granitic rocks. Journal of Petrology, 25(4), 956-983.

Quesada, C., Cueto, L.A., Dallmeyer, R.D., 1989. Nuevas dataciones absolutas en la Zona de Ossa Morena: limitaciones que se imponen a la evolución tectónica de la misma. XI Reunión Xeoloxia e Mineria do Noroeste Peninsular, Santiago de Compostela, España, 35-36.

Rubio Ordóñez, A, Valverde-Vaquero, P, Corretgé, L.G., Cuesta-Fernández, A., Gallastegui, G., Fernández-González, M., Gerdes, A., 2012. An Early Ordovician tonalitic-granodioritic belt along the Schistose-Greywacke Domain of the Central Iberian Zone (Iberian Massif, Variscan Belt). Geological Magazine, 149(5), 927-939.

Schermerhorn, L.J.G., 1971. An outline stratigraphy of the Iberian Pyrite Belt. Boletín Geológico y Minero, 82, 239-268.

Schütz, W., Ebneth, J., Meyer, K.D., 1987. Trondhjemites, tonalites and diorites in the South Portuguese Zone and their relations to the vulcanites and mineral deposits of the Iberian Pyrite Belt. Geologische Rundschau, 76(1), 201-212.

Simancas, J.F., 1981. Plutonismo ácido y básico en el extremo oriental de la Zona Sudportuguesa. Cuadernos Geología Ibérica, 7, 309-326.

Simancas, J.F., 1983. Geología de la extremidad oriental de la Zona Sudportuguesa. Doctoral Thesis, Universidad de Sevilla, 439pp.

Sun, S., McDonough, W.F., 1989. Chemical and isotopic systematics of oceanic basalts: implications for mantle composition and processes. In: Saunders, A.D., Norry, M.J. (eds.). Magmatism in the Ocean Basins. Geological Society, London, Special Publications, 42, 313-345.

Valverde-Vaquero, P., 2009. Método de datación U-Pb ID-TIMS en el laboratorio geocronológico del IGME (Tres Cantos). VII Congreso Ibérico de Geoquímica, Tres Cantos, Madrid, 758-765.

Villaseca, C., Pérez-Soba, C., Merino, E., Orejana, D., López-García, J.A., Billstrom, K., 2008. Contrasting crustal sources for peraluminous granites of the segmented Montes de Toledo Batholith (Iberian Variscan Belt). Journal of Geosciences, 53, 263-280.

von Raumer, J.F., Stampfli, G.M., Bussy, F., 2003. Gondwana-derived microcontinents – the constituents of the Variscan collision orogens. Tectonophysics, 365, 7-22.